Observation of McMillan-Rowell like oscillations in underdoped $YBa_2Cu_3O_y$ junctions oriented along the node of the *d*-wave order parameter

L. Shkedy, P. Aronov,* G. Koren, and E. Polturak
Physics Department, Technion-Israel Institute of Technology, Haifa 32000, Israel
(Received 27 August 2003; revised manuscript received 26 November 2003; published 26 April 2004)

Dynamic resistance spectra of ramp type junctions made of underdoped $YBa_2Cu_3O_y$ (YBCO) electrodes and Ga-doped YBCO barrier are reported. Series of equidistant peaks were observed in these spectra in junctions oriented along the node direction. Junctions with different barrier thickness d_N showed that the distance between adjacent peaks scales inversely with d_N. The peaks were thus identified as due to McMillan-Rowell like oscillations in the barrier. Analysis of the series of peaks yields an upper limit of about 3.7 meV on the value of the energy gap along the node. We attribute this small gap to the is component of the order parameter of underdoped YBCO near the interface of the junctions.

DOI: 10.1103/PhysRevB.69.132507 PACS number(s): 74.20.Rp, 74.50.+r, 74.72.Bk

Several experiments show that the dominant component of the order parameter in the high-temperature superconductors (HTS) has a $d_{x^2-y^2}$-wave symmetry.[1] Other experiments are consistent with the existence of an additional subdominant component on the surface of the HTS, of is or id_{xy} wave nature.[2–6] It should be stressed though that bulk measurements such as thermal conductivity and specific heat show no sign of a subdominant component in the order parameter of the cuprates.[7,8] Tunneling measurements of underdoped junctions show that in addition to the $d_{x^2-y^2}+is$ gap, a large gap which can be attributed to the pseudogap is also present.[9–11] The magnitude of the is component was found to be quite small, in the range of 1–3 meV.[2–6] Recent self-consistent calculations using Bogoliubov–De Gennes type equations led to a good fit of the data assuming a pure *d*-wave symmetry in the bulk, and coexistence of $d_{x^2-y^2}$ and *is* order parameters near the interface.[12] The magnitude of the *is* gap resulting from these simulations is 2.6 ± 0.1 meV. In the present experiment we observed series of geometrical resonances in the dynamic resistance spectra of node junctions. From these series, we find an upper limit of 3.7 meV on the energy of the subdominant *s*-wave component of the gap, which is consistent with the simulations results.

In the present study we used ramp type junctions with a Ga-doped $YBa_2Cu_3O_y$ (YBCO) barrier instead of the Fe-doped YBCO barrier used before.[5,6,11,13,14] This was done in order to check if the appearance of an *is* gap depends on the nature of the barrier. In particular, magnetic effects in the barrier are not likely to be the source of this gap, if found in both types of junctions. Figure 1 shows the resistivity versus temperature of a blanket $YBa_2Ga_{0.4}Cu_{2.6}O_y$ film deposited on (100) $SrTiO_3$ (STO) wafer, annealed *in situ* under the same annealing conditions as for obtaining YBCO films with $T_c = 60$ K. This barrier material behaves like a Mott insulator (MI) with variable range hopping (VRH) in three-dimensions with $\ln(\rho) \propto T^{-1/4}$ for the whole temperature range. The resistivity value at 2 K is of about 0.6 Ω cm, which is more than an order of magnitude higher than that of $YBa_2Fe_{0.45}Cu_{2.55}O_y$ used previously as the barrier layer.[14] The geometry of the junction is described schematically in the inset of Fig. 1. All the YBCO and doped YBCO layers are epitaxial with the *c* axis normal to the wafer. The two superconducting YBCO electrodes are coupled in the *a-b* plane via a thin barrier layer of the Ga-doped YBCO film.

The multistep junction preparation process was described before.[13] Briefly, we first prepared by laser ablation deposition the base electrode, which was composed of a bilayer of STO on YBCO on (100) STO wafer. Patterning of the base electrode was done by photolithography and Ar ion beam milling. The ramps of the junctions were patterned along the node direction of the YBCO film. After a thorough cleaning process, the cover electrode was deposited. This included the barrier layer, a second YBCO film, and an Au layer on top. The cover electrode was then patterned to produce the final junction layout, as well as the four gold pads for each junction. All junctions in the present study had the same 90 nm thick YBCO electrodes (base as well as cover), the same lateral width of 5 μm, and varying barrier thickness. The resistance versus temperature of the junctions was measured using the standard four probe technique, and the dynamic resistance was measured using a standard ac modulation technique.

Figure 2 shows the measured resistance as a function of temperature of three node junctions with 10.5, 21, and 32 nm thick barriers. The corresponding normal state resistance of these junctions is typical of underdoped $YBa_2Cu_3O_y$ with *y*

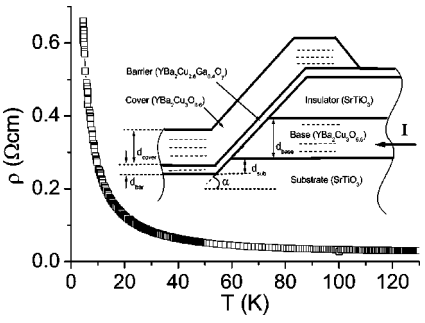

FIG. 1. Resistivity vs temperature of a Ga-doped YBCO film. The resistivity values were obtained by averaging over six microbridges which were patterned in an 80 nm thick film. The inset shows a schematic cross section of a ramp type junction.

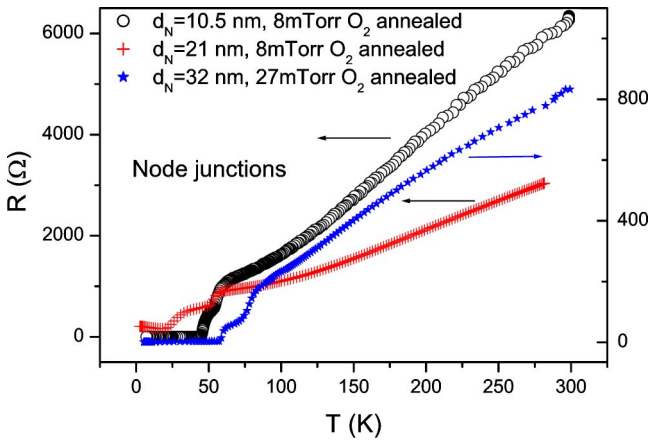

FIG. 2. (Color online) Resistance vs temperature of three node junctions with 10.5, 21, and 32 nm thick Ga-doped YBCO barrier. The junction with the 10.5 nm thick barrier had longer leads which led to a higher normal resistance.

$\sim$6.55 for the 8 mTorr oxygen annealed ones and $y \sim 6.85$ for the 27 mTorr oxygen annealled junction.[15] One can observe two distinct transitions in the resistance of each junction. In the two oxygen deficient junctions (8 mTorr annealing), the transition temperature T_c of the electrodes occurs at approximately 55 K, while in the third oxygen rich junction (27 mTorr annealing) the electrodes become superconducting already at 80 K. The transitions seen at 40 and 25 K in the first two junctions, and at 60 K in the third one, result presumably from an apparent proximity effect in the barrier. At low temperatures, the junction with the 10.5 nm thick barrier shows a critical current of about 0.5 mA at 5 K which yields a critical current density of $\sim 1.1 \times 10^4$ A/cm^2. The other two junctions with the 21 and 32 nm thick barriers are resistive at low temperatures and have resistance values at low bias of about 200 and 2Ω, respectively.

The dynamic resistance spectra of the two oxygen deficient node junctions with 21 and 10.5 nm thick barriers are shown in Figs. 3 and 4, respectively. The different behavior at low bias, namely, tunneling like in Fig. 3, and critical current and zero-bias conductance peak (ZBCP) in Fig. 4, is

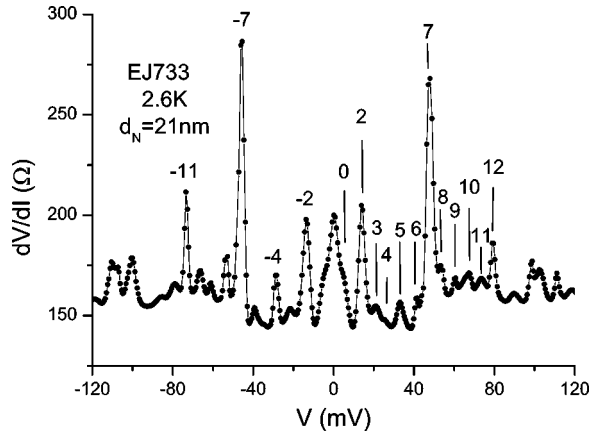

FIG. 3. Dynamic resistance spectra of the junction in Fig. 2 with the 21 nm thick barrier.

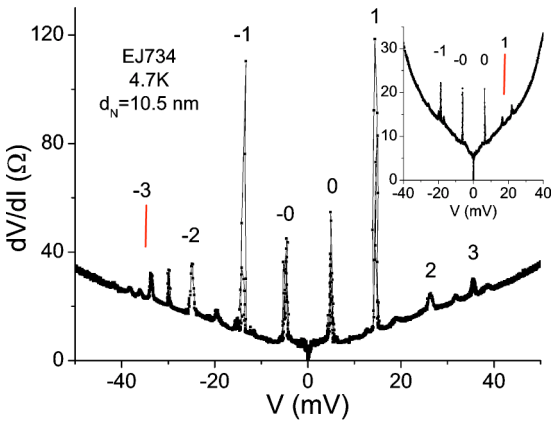

FIG. 4. (Color online) Dynamic resistance spectra of the junction in Fig. 2 with the 10.5 nm thick barrier (three traces, main panel, peak no. -3 is missing). In the inset, the results of another node junction on the same wafer are shown (two traces, peak no. 1 is missing).

due to the much higher normal resistance of the first junction [R_N (3 K)$\sim$200 Ω]. A third junction with a 32 nm thick barrier was annealed in a higher oxygen pressure of 27 mTorr in order to avoid a very high R_N (5 K). The dynamic resistance spectra of this junction (not shown) was similar to that of Fig. 3, but with a ZBCP and a more closely spaced series of peaks. In all three junctions, the peaks bias in the dynamic resistance spectra seem to be almost independent of the oxygen content, or the presence of a ZBCP. It was, however, strongly dependent on the thickness of the barriers. It is generally nontrivial to associate a peak number to each peak in the series because not all of them are present or have the same intensity. By comparison, however, with data of other node junctions, we could determine the peak numbers properly, and in Fig. 5 we plot the corresponding voltage values of four series versus the peak number including the data of Figs. 3 and 4. Figure 5 shows that each series of peaks appears with a constant voltage difference between adjacent peaks, and includes linear fits of the data. Figure 5 also shows that the ratio of adjacent peaks spacing in the three types of junctions 10.1–12:6.5:4.5 is approximately equal to

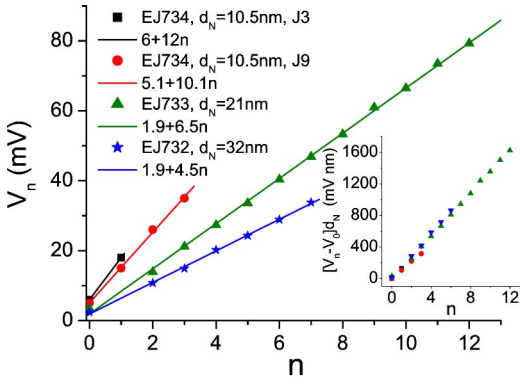

FIG. 5. (Color online) Peak voltages of the series in Figs. 3 and 4 vs the peak number, together with the series of peaks of the oxygen rich junction in Fig. 2 with the 32 nm thick barrier. The straight lines are linear fits to the data. Scaling of all series with the barrier thickness is demonstrated in the inset.

the inverse ratio of the corresponding barrier thicknesses (1/10.5):(1/21):(1/32). Since the superconducting electrodes in all our junctions have the same 90 nm thickness, the above result seems to indicate that the series of peaks in the dynamic resistance spectra originate in geometrical resonances in the barrier layer. Next we discussed this result in the context of the nature of the present S/MI/S junctions (MI is a Mott insulator with VRH).

It has already been demonstrated in the past that *a* axis YBCO/$PrBa_2Cu_3O_{7-\delta}$/YBCO junctions which are basically S/MI/S junctions as we have here, carry significant critical currents I_c at low temperatures even when the barriers are up to 100 nm thick.[16] Surprisingly for this kind of junctions, it was found that $I_c(T)$ behaves as $\exp[-aT^{0.5}]$, where a is a constant, which is exactly the expected behavior for SNS type junctions with a normal metal barrier in the dirty limit. In ramp type junctions with $PrBa_2Cu_{2-x}Ga_xO_{7-\delta}$ barrier, however, no such temperature dependence was found.[17] In this case, the transport results point to tunneling, but this seems to be due to the much higher resistivity of the barrier at low temperatures ($\sim 10^3\ \Omega$ cm) as compared with 0.5 Ω cm in Ref. 16 which is closer to the resistivity value in the present study. There are many more reports on observations of a long-range proximity effect and Andreev reflections in similar type of junctions with insulating VRH barriers.[14,18–20] The puzzling question is why such barrier materials with a resistivity of two to three orders of magnitude higher than ~ 1 mΩ cm the maximum resistivity a metal can have, when in contact with a superconductor should behave like normal metals? This is a complicated problem to deal with theoretically, and only sketchy reports on this issue exist.[21] We shall not attempt to speculate what is the reason for this normal metal-like behavior of the VRH barriers in the S/MI/S junctions, but simply take it as given, and use the formulas derived for SNS junctions.

Geometrical resonances in NS bilayers can lead to series of peaks in the dynamic resistance spectra. Subgap series involve subharmonic resonances, which are caused by multiple Andreev reflections, and de Gennes–Saint James bound states.[14,22,23] Both result in series of peaks which are not equally spaced, and therefore cannot account for the present observations. Above gap resonances involve Tomasch and McMillan-Rowell oscillations.[24,25] Tomasch oscillations are due to resonances in the superconducting electrode, of which peak energies are given by

$$eV_n = \sqrt{(2\Delta)^2 + \left[\frac{nhv_{FS}}{2d_S}\right]^2}, \qquad (1)$$

where Δ is the gap energy, v_{FS} is the Fermi velocity in the S electrode, d_S is the S electrode thickness, and n is the peak number. These resonances are not equally spaced, but for a small node gap value the deviation from equal spacing is quite small, and generally cannot be observed due to the experimental error. McMillan-Rowell oscillations (MRO), (Ref. 25) are also seen as series of equidistant peaks in the dynamic resistance spectra, and are caused by geometrical resonances in the normal metal. The voltage difference between adjacent peaks in this case is

$$\Delta V = \frac{hv_{FN}}{4ed_N}, \qquad (2)$$

where v_{FN} is the Fermi velocity in the normal metal, and d_N is the N layer thickness. Thus both Tomasch and McMillan-Rowell like oscillations can yield a linear behavior of the peak voltage versus peak number as seen in Fig. 5. For SNS junctions Eqs. (1) and (2) should be modified because of Andreev scattering at both interfaces. The oscillation periods should thus be twice as large: hv_{FS}/d_S for the Tomasch oscillations and $hv_{FN}/2d_N$ for the MRO case.

The voltage difference between adjacent peaks in the dynamic resistance spectra, depends on either the thickness of the superconducting electrode in the Tomasch scenario as seen in Eq. (1), or on the barrier thicknesses in the MRO case as seen in Eq. (2). Since the thicknesses of the superconducting base and cover electrodes are *the same* for all our junctions, and the observed series of peaks depend on the thickness of the barrier as seen in Fig. 5, it seems that these series are due to MRO. Moreover, Fig. 5 shows scaling with the barrier thickness d_N as depicted by Eq. (2). The fact that all data points in the inset of Fig. 5 fall on a single straight line further supports the identification of the observed resonances as due to MRO. We stress that this result is independent of either the barrier strength or the different oxygen content of the junctions. Using Eq. (2) we find an effective Fermi velocity of electrons in the barrier $v_{FN} = 1.2 \pm 0.2 \times 10^7$ cm/sec, which compares well with a previous result of 1.5×10^7 cm/sec measured in the same kind of junction with a Fe-doped YBCO barrier.[14] The latter has a much lower resistivity value at low temperatures, of the order of 10–20 mΩ cm, thus being much closer to a normal metal than the present Ga-doped YBCO. *A priori* the Fermi velocity is not well defined here since there is no Fermi surface at all in isolated VRH materials. When the thin VRH layer, however, is in contact with a superconductor like in the present junctions, it is possible that the Fermi surface is recovered, and the Fermi velocity is thus well defined. The fact that similar numbers were obtained for v_{FN} of the Fe- and Ga-doped YBCO barriers which have very different resistivity values, further supports the notion that the barrier in S/MI/S junctions have *N*-like features. Our effective v_{FN} values are quite smaller than the value $v_F \approx 2.5 \times 10^7$ cm/sec obtained by angle-resolved phtoemission spectroscopy along the node direction in differently doped $La_{2-x}Sr_xCuO_4$ (LSCO) crystals.[26] This ARPES study, however, shows that there is no direct link between the measured Fermi velocity in the cuprates and the magnitude of the resistivity. A serious theoretical analysis of these issues is thus needed.

The voltage values at $n=0$ in Fig. 5 constitute an upper limit on the energy gap value. Previous MRO results yielded an $n=0$ value of 16 mV along the main crystallographic axis, which is an upper limit on the value of the dominant *d*-wave component of the gap in the 55 K phase of YBCO.[14] In the present study, on the contrary, the junctions are aligned along the node direction where the dominant *d*-wave gap vanishes. We can thus measure an upper limit on the energy gap of the subdominant component by taking the average value of the intercepts at $n=0$ of the four straight lines in

Fig. 5. This yields an upper limit of 3.7 mV on the energy of the *s* gap near the interface, which is in reasonable agreement with the measured gap values of 2.5 ± 0.5 meV found previously.[5,6]

In summary, the present study shows that the experimental properties of S/MI/S junctions made of underdoped YBCO have several common features with conventional SNS junctions. Measurements of dynamic resistance spectra in underdoped YBCO junctions along the node direction show geometrical resonances in the barrier which behave like McMillan-Rowell oscillations above the gap. From these we find an upper limit of 3.7 meV on the magnitude of the *is* component of the gap near the interface.

This research was supported in part by the Israel Science Foundation, the Heinrich Hertz Minerva Center for HTSC, the Karl Stoll Chair in advanced materials, and by the Fund for the Promotion of Research at the Technion.

*Corresponding author. Electronic address: gkoren@Physics.technion.ac.il

[1] C.C. Tsuei and J.R. Kirtley, Rev. Mod. Phys. **72**, 969 (2000).
[2] M. Covington, M. Aprili, E. Paraoanu, L.H. Greene, F. Xu, J. Zhu, and C.A. Mirkin, Phys. Rev. Lett. **79**, 277 (1997).
[3] R. Krupke and G. Deutscher, Phys. Rev. Lett. **83**, 4634 (1999).
[4] A. Sharoni, G. Koren, and O. Millo, Europhys. Lett. **54**, 675 (2001).
[5] G. Koren and N. Levy, Europhys. Lett. **59**, 121 (2002).
[6] G. Koren, N. Levy, and E. Polturak, J. Low Temp. Phys. **131**, 849 (2003).
[7] M. Sutherland *et al.*, Phys. Rev. B **67**, 174520 (2003).
[8] K.A. Moler, D.J. Baar, J.S. Urbach, R. Liang, W.N. Hardy, and A. Kapitulnik, Phys. Rev. Lett. **73**, 2744 (1994).
[9] G. Deutscher, Nature (London) **397**, 410 (1999).
[10] V.M. Krasnov, A. Yurgens, D. Winkler, P. Delsing, and T. Claeson, Physica C **352**, 89 (2001); and V.M. Krasnov, A.E. Kovalev, A. Yurgens, and D. Winkler, Phys. Rev. Lett. **86**, 2657 (2001).
[11] G. Koren, L. Shkedy, and E. Polturak, Physica C **403**, 45 (2004).
[12] I. Lubimova and G. Koren, Phys. Rev. B **68**, 224519 (2003).
[13] O. Nesher and G. Koren, Appl. Phys. Lett. **74**, 3392 (1999).
[14] O. Nesher and G. Koren, Phys. Rev. B **60**, 9287 (1999).
[15] Y. Ando and K. Segawa, Phys. Rev. Lett. **88**, 167005 (2002).
[16] T. Hashimoto, M. Sagoi, Y. Mizutani, J. Yoshida, and K. Mizushima, Appl. Phys. Lett. **60**, 1756 (1992).
[17] M.A.J. Verhoeven, G.J. Gerritsma, H. Rogalla, and A.A. Golubov, Appl. Phys. Lett. **69**, 848 (1996).
[18] U. Kabasawa, Y. Tarutani, M. Okamoto, T. Fukazawa, A. Tsukamoto, M. Hiratani, and K. Takagi, Phys. Rev. Lett. **70**, 1700 (1993).
[19] C. Stozel, M. Siegel, G. Adrian, C. Krimmer, J. Sollner, W. Wilkens, G. Schulz, and H. Adrian, Appl. Phys. Lett. **63**, 2970 (1993).
[20] A. Frydman and Z. Ovadyahu, Europhys. Lett. **33**, 217 (1996).
[21] Y. Tanaka, *Coherence in High Temperature Superconductors*, edited by G. Deutscher and A. Revcolevschi (World Scientific, Singapore, 1995), pp. 393–411.
[22] A.F. Andreev, Zh. Eksp. Teor. Fiz. **46**, 1823 (1964) [Sov. Phys. JETP **19**, 1228 (1964)].
[23] P.G. de Gennes and D. Saint-James, Phys. Lett. **4**, 151 (1963).
[24] W.J. Tomasch, Phys. Rev. Lett. **15**, 672 (1965); **16**, 16 (1966); W.L. McMillan and P.W. Anderson, *ibid.* **16**, 85 (1966).
[25] J.M. Rowell and W.L. McMillan, Phys. Rev. Lett. **16**, 453 (1966).
[26] Z.X. Shen, cond-mat/0305576 (unpublished).